Applied Geochemistry 204 (2026) 106838

Contents lists available at ScienceDirect

Applied Geochemistry

journal homepage: www.elsevier.com/locate/apgeochem

Metal contaminant availability in freshly dredged sediments and controlling reactive mineral and organic surfaces

Maarten C.J.M. Van Hoef [a,*], Joris J. Dijkstra [b,a], Rob N.J. Comans [a]

[a] *Soil Chemistry Group, Wageningen University & Research, P.O. box 47, Wageningen, 6700 AA, the Netherlands*

[b] *Geological Survey of the Netherlands, Netherlands Organisation for Applied Scientific Research (TNO), Princetonlaan 6, Utrecht, 3508 TA, the Netherlands*

ARTICLE INFO

Editorial handling by Elisa Sacchi

Keywords:
Sediment ripening
Geochemical modelling
Metal contamination
pH-dependent solubility
Metal hydroxides
Organic matter

ABSTRACT

In this paper we evaluate the environmental and geochemical properties of freshly dewatered dredged sediment at the start of a multiyear field-scale ripening experiment designed to obtain suitable material for construction. The solid-solution partitioning of metal(loid) contaminants was determined over a wide pH-range and related to the binding properties of natural reactive mineral and organic surfaces in the sediment. The results were interpreted using a multisurface geochemical model, comparing partitioning with the 'generalised two layer model' (GTLM) and 'charge distribution and multisite ion complexation' (CD-MUSIC) submodels, which differ in the level of detail for adsorption of major and minor ions to Fe- and Al-(hydr)oxides. The measured and modelled solubility of metal(loid)s varied by several orders of magnitude across the pH-range, often with a minimum around neutral pH. Surface characterisation showed a high reactive surface area for the metal (hydr)oxides and a low organic matter reactivity for metal binding, in contrast to terrestrial soils. Consequently, the adsorption to metal (hydr)oxides was dominant in the modelled speciation of several metal(loid) contaminants. Despite this importance of metal (hydr)oxides, only minor differences were found between the solid-solution partitioning predicted using the GTLM and the CD-MUSIC submodels. Therefore, the predicted solid-solution partitioning did not fully reflect the benefits offered by the more mechanistic CD-MUSIC model for contaminant adsorption to metal (hydr)oxides in the sediment. We conclude it is rather the conceptual framework of the CD-MUSIC model which, when combined with independent information from surface characterisation and pH-dependent extractions, contributes to understanding contaminant behaviour in the freshly dredged sediment.

1. Introduction

Waterways and ports are dredged to ensure accessibility and to improve water quality. Worldwide, dredging results in a vast amount of sediment that is disposed (Balkaya, 2018; OSPAR, 2017). However, these sediments hold valuable potential for sustainable applications instead of disposal, especially considering the increasing demand for mineral construction material (CEDA, 2019; Crocetti et al., 2022). Contamination by metal(loid)s can hamper the suitability of sediments for application, because it poses risks for human health and environmental safety. The risks associated with the presence of contaminants depend strongly on their solid-solution partitioning rather than their total concentrations (Harmsen, 2007). Sediments contain natural reactive surfaces such as clay, sulphides, organic matter (OM), and Fe- and Al-(hydr)oxides, which are able to adsorb metal(loid)s and impact the solid-solution partitioning of these contaminants (Haynes and Zhou, 2022). Other geochemical processes, such as mineral precipitation and solution speciation, together with adsorption to reactive surfaces govern the transport and bioavailability of metal(loid)s (Tipping et al., 2003; Kim et al., 2015). Thus, a better understanding of the properties of reactive surfaces and the above mentioned geochemical processes may contribute to a treatment and utilisation approach that reduces risks and improves the usability of dredged sediments.

In general, sediments are not suitable for application directly after dredging. In many cases dewatering and aeration followed by ripening, is required to improve physico-chemical and structural stability of the sediment. During ripening physical, chemical, and biological processes take place that ultimately transform a sediment into a soil (Vermeulen et al., 2003). The transition from anaerobic to aerobic conditions alters the chemical speciation of contaminants in the system (Vermeulen et al., 2007). Aerobic conditions also cause (trans)formation of reactive surfaces as sulphides are oxidised and Fe- and Al-(hydr)oxides are formed

---

* Corresponding author.
E-mail address: maarten.vanhoef@wur.nl (M.C.J.M. Van Hoef).

https://doi.org/10.1016/j.apgeochem.2026.106838
Received 21 October 2025; Received in revised form 2 April 2026; Accepted 17 April 2026

upon aeration (Caille et al., 2003; Vermeulen et al., 2003) and the composition of OM is altered (Oliveira et al., 2016; Liu et al., 2021). The solid-solution partitioning of contaminants changes over time as a consequence of the changing chemical speciation and the (trans)formation of reactive surfaces. As sediments can undergo a strong shift in chemical conditions after dredging, the fate of contaminants requires special attention in ripening sediments.

The solid-solution partitioning of metal(loid)s in a batch experiment can be used to estimate the availability of contaminants in the field. This partitioning strongly depends on pH in a wide variety of matrices (Dijkstra et al., 2006; Frémion et al., 2017; Van Raffe et al., 2025). Thus, pH-controlled batch experiments can provide valuable insights beyond the solubility at the natural pH of the sample (Dijkstra et al., 2006). By considering a wide pH-range (i.e., 2-12) chemical processes are more comprehensively highlighted, which facilitates their identification. Observed pH-dependent concentration trends can be linked to fundamental processes by using geochemical models (Groenenberg and Lofts, 2014). Combining pH-dependent solid-solution partitioning experiments with geochemical models holds potential to assess the speciation and behaviour of contaminants in ripening sediments. In addition, the leaching potential can be evaluated for different environmental scenarios that may occur during ripening.

The experimentally determined solid-solution partitioning of metal contaminants can be related to independently determined estimates of the amount and reactivity of the organic and metal (hydr)oxide reactive surfaces (Groenenberg et al., 2012). Over the past decades several techniques have been developed to quantify natural reactive surfaces as well as to characterise their adsorption properties. Extraction-based definitions of natural OM fractions and metal (hydr)oxides have been applied effectively to a variety of environmental samples (Weng et al., 2001; Ren et al., 2015; Van Raffe et al., 2025). The adsorption properties of solid and dissolved OM can be characterised by operationally defined fractions of ‘humic substances’ based on hydrophobicity and (de)protonation behaviour (Swift, 1996; Van Zomeren and Comans, 2007). Because the origin and prior degradation of OM in sediments differ from that in soils (Bastviken et al., 2004; Liu et al., 2021), common assumptions about the amount of OM that is active in adsorption processes may not be applicable for freshly dredged sediment. Metal (hydr)oxides are often quantified by selective extractions targeting different levels of (hydr)oxide crystallinity (Kostka and Luther, 1994). The total reactive surface area (RSA) of metal (hydr)oxides can be estimated from the operationally defined crystallinity and an assumed specific surface area (SSA) (e.g., Dzombak and Morel, 1990). However, the effective RSA can also be determined experimentally in environmental samples (Hiemstra et al., 2010). The environmental conditions are likely to affect the (trans)formation and consequently the reactive properties of metal (hydr)oxides (Jones et al., 2009; Chen and Thompson, 2017). Indeed, the measurements of the SSA differ substantially between soils and a generic value may thus misrepresent the specific reactivity of the metal (hydr)oxides, especially considering the different nature of sediment (-like) material from soils (Mendez et al., 2020).

Mechanistic modelling of adsorption phenomena has become key in relating the solid-solution partitioning of metals to the presence, nature, and amount of reactive surfaces (Groenenberg and Lofts, 2014). Specifically multisurface geochemical models have been shown to enable adequate predictions of the geochemical behaviour and solubility of many metal(loid) contaminants in a variety of environmental systems (Groenenberg and Lofts, 2014). These models can combine solution speciation, mineral formation, and adsorption to OM, metal (hydr)oxides, and clay. Within a multisurface model, the total adsorption is determined as the linear addition of adsorption derived by specific submodels for each surface. The submodels describe adsorption to a surface using generic binding parameters and are thus independent of the data that is evaluated (e.g., Dijkstra et al., 2009). The evaluation of experimental measurements of solid-solution partitioning by geochemical modelling depends on (i) a proper description of the surfaces to which contaminants may adsorb and (ii) an adequate adsorption model for each of these surfaces. The ‘generalised two layer model’ (GTLM) of Dzombak and Morel (1990) and the ‘charge distribution and multisite ion complexation’ (CD-MUSIC) model of Hiemstra and Van Riemsdijk (1996, 2009) have both been used to model adsorption to metal (hydr)oxides. However, these two models differ greatly with respect to the level of detail at which fundamental molecular and electrostatic interactions are implemented.

In this paper we present the geochemical characterisation of dredged sediment one month after the start of an approximately three year field-scale ripening experiment. This ripening experiment was designed to study ripening processes over a time period and on a scale that are relevant to obtain a suitable material for application in construction. The environmental quality and stability of the dredged sediment are studied during the ripening process under different stockpiling practices (i.e., turning frequency and the removal of vegetation). Within this context, we (i) experimentally assess the pH-dependent contaminant solid-solution partitioning, (ii) characterise the reactive surface compounds present in the sediment, and (iii) model the obtained solid-solution relationships with the characterised reactive surfaces based on their generic binding parameters. In this work, we put particular emphasis on the importance of the sediment-specific binding properties of reactive mineral and organic surfaces, and the associated choice of their representative geochemical submodels for the accuracy of predicting contaminant solid-solution partitioning. As the binding properties of reactive surfaces in the freshly dredged sediment may differ from those in soils, we include surface specific techniques to parameterise these models, such as the determination of the RSA according to Hiemstra et al. (2010) and quantification of the humic fractions described by Van Zomeren and Comans (2007). A particular novelty of this study is that we compare two widely used, but mechanistically different approaches to describe adsorption to metal (hydr)oxides, namely GTLM and CD-MUSIC. To our knowledge, no comparison has been made so far between these two models with respect to their performance in a real environmental system with multiple metal(loid) contaminants. With this approach, we assess the appropriateness of recent characterisation methods developed mostly for soils and geochemical models in the novel context of studying contaminant behaviour in dredged sediments during ripening. As such, this study provides a benchmark for future investigations into the availability of contaminants and the (trans)formation of reactive surfaces during further ripening in the field.

2. Methods and materials

2.1. Sampling

The sampled sediment was originally dredged from the Elbe river in the Port of Hamburg and stored submerged in a flushing basin. The sand fraction was removed and the residual dredged sediment was partially dewatered in the METHA plant, which takes approximately 24 h combined (Detzner et al., 1998). Nine stockpiles (approximately 2 m high, 4 m wide, and 200 m long) were made of the dredged sediment's dewatered finer fraction in December 2022. The sampling of stockpiled dredged sediment was done in January 2023 in Hamburg, Germany. A detailed description of METHA treatment and stockpiling is given in Section S1. Samples were taken over a depth of 0-1.2 m by excavation in the middle of eight stockpiles and ten times along a transect for one stockpile. All sampled material was sieved over 4 mm before further analyses. A mixed sample was made, based on equal amounts of dry weight, from six selected stockpiles to represent the initial (t_0) composition of the stockpiled dredged sediment. The field moist samples were stored in the dark in sealed containers at 4 °C.

2.2. General characterisation of the stockpiled sediment

The heterogeneity both within the single stockpile transect and between the different stockpiles was assessed by measurements of pH, electrical conductivity (EC), water content (θ), and loss on ignition (LOI) of the individual samples, details for which are given in Section S2. All further characterisation was done using field moist material converted to dry weight by their water content. The 'total' reactive amount of elements was determined by an extraction with 0.43 M HNO_3 at a liquid/solid (L/S) ratio of 10 (ISO 17586, 2016). An additional 0.20 mL 5 M HNO_3 was added for each % of $CaCO_3$ present in the samples based on total inorganic C (IC). After 4 h of horizontal shaking the suspensions were centrifuged at 3000 g for 10 min and filtered with 0.45 μm membrane filters. The elemental concentrations of Al, As, Ba, Ca, Cd, Co, Cr, Cu, Fe, K, Mg, Mn, Mo, Na, Ni, P, Pb, S, Sb, Sn, Sr, and Zn were measured by inductively coupled plasma – optical atomic emission spectroscopy (ICP-OES - *iCAP 6500 DUO, Thermo Fisher Scientific Inc., Waltham, USA*) and high resolution inductively coupled plasma – mass spectrometry (ICP-MS - *Element 2, Thermo Fisher Scientific Inc., Waltham, USA*). The concentration of major and trace elements extracted by 1 mM $CaCl_2$ (L/S 10) similar to ISO 21268-2 (2019), with an exception to the filter-size used, was considered a proxy for their directly available amount. The suspensions were shaken horizontally for 24 h in closed centrifuge tubes. The suspensions were then centrifuged for 30 min at 3000 g and filtered with 0.45 μm membrane filters. After acidification with HNO_3, the concentration of metal(loid)s, S, and P was determined the same way as for the 0.43 M HNO_3 extractions. The solution concentration of IC, total C, NH_4, NO_2+NO_3, and total N were measured with a segmented flow analyser (SFA - *SAN++, Skalar, Breda, NL*).

2.3. Characterisation of reactive surfaces

The total (elemental) amounts of solid IC, C, and N were measured with an elemental analyser (*CN828, LECO, St Joseph, USA*). The 'reactive' OM in the samples was characterised by fractionation of humic substances as described in ISO 12782-4 (2012). The extracted total (acid-base) OM and the dissolved OM in the pH-stat solutions (Section 2.4) were separated into operationally defined humic acids (HA), fulvic acids (FA), hydrophilic acids (Hy), and hydrophobic neutrals (HON). The organic carbon (OC) concentrations in the separated fractions were determined by SFA.

Quantification of Fe-, Al-, and Mn (hydr)oxides with different levels of crystallinity was done by selective extraction with ascorbic acid, ammonium oxalic acid, and sodium dithionite citric acid. All three extractions were done according to the respective ISO standards (ISO 12782-1, 2012; ISO 12782-2, 2012; ISO 12782-3, 2012) - a brief description is given in Section S2. The concentrations of Fe, Al, Mn, and co-extracted P were measured by ICP-OES.

The combined RSA of the metal (hydr)oxides was assessed with the probe-ion method of Hiemstra et al. (2010). In short, extractions with 0.5 M $NaHCO_3$ adjusted to pH 8.5 were done at an L/S of 5, 20, 50, 100, and 200. Pre-cleaned activated carbon (0.4 g/g soil) was added to the samples to prevent interaction with dissolved OM (Mendez et al., 2020). The samples were shaken end-over-end for 14 days to reach (semi-) equilibrium (Hiemstra et al., 2010). The inorganic orthophosphate (PO_4) concentration in all extracts was measured colorimetrically by a discrete analyser (*BLUVISION, Skalar, Breda, NL*). The obtained desorption isotherm of PO_4 was used to fit the reversibly bound PO_4 and the RSA. The fitting procedure made use of specific sorption of PO_4^{3-} and HCO_3^- to ferrihydrite (Fh) with the CD-MUSIC model equal to Mendez et al. (2020), who have also verified the suitability of using Fh as a proxy to derive the RSA of metal (hydr)oxides in soils.

2.4. pH dependent solubility of contaminants and surfaces

The pH-dependent solid-solution partitioning of elements in the t_0 mixed sample was assessed by static pH (pH-stat) extractions targeting a distinct pH ranging from 2 to 12, largely according to NEN-EN 14997 (2015). In short, the pH in eight parallel stirred PTFE reaction vessels was continuously measured and adjusted by addition of HCl or NaOH (Meima and Comans, 1999). One extraction was conducted without acid or base dosage, i.e., at the natural pH. The extraction at natural pH and a blank extraction (without sediment) were done in identical reaction vessels as the pH-stat extractions. All extractions were done in ultrapure water (UPW) or 1 mM $CaCl_2$ at an L/S of 10. The pH-stat extraction was originally performed with UPW, eight months later an additional pH-stat experiment was performed on stored sediment using 1 mM $CaCl_2$. The suspensions had free interaction with the atmosphere, in line with the oxic character of the sediment considering the METHA-treatment and subsequent stockpiling. After 48 h the final pH and pe were determined and thereafter the suspensions were centrifuged for 10 min at 3000 g or 10000 g for samples with a high dissolved OM content. After centrifugation, samples were filtered using 0.45 μm membrane filters. The concentrations of 20 metals, S, P, IC, C, NH_4, NO_2+NO_3, and total N were all determined equal to the 24 h 1 mM $CaCl_2$ batch extractions (Section 2.2).

2.5. Geochemical modelling

Geochemical modelling was performed within the ORCHESTRA framework (Meeussen, 2003). For each 1 mM $CaCl_2$ pH-stat extraction, the solution speciation, mineral precipitation, and adsorption to Fe- and Al-(hydr)oxides, OM, and clay were calculated for all measured elements. Solution speciation and mineral precipitation were calculated using the reaction equations and equilibrium constants from the MINTEQ database (US-EPA, 1999). Additionally, the solubility product of willemite (Zn_2SiO_4) was taken from Ball & Kirk Nordstrom (2001). The included precipitates are given in Table S5. The submodels for adsorption are presented below. The pH and pe that were measured at the end of the 48 h batch experiment were used as input for each extraction. The pH + pe varied between 13 at low and 17 at high pH, indicating mildly oxidising conditions. The total reactive concentration, as determined by the 0.43 M HNO_3 extraction was used as input for the total concentration of each modelled element. The model-predicted pH-dependent solution concentrations were evaluated against the measured solution concentrations from the pH-stat experiment. Instead of calculating the solution concentrations of all target elements simultaneously, as done in e.g., Dijkstra et al. (2004, 2009), the 'total' reactive amount of only one element at a time was used as model input, as done in e.g., Van Raffe et al. (2025). The concentrations of all other elements were fixed at their measured solution concentrations at each pH, whilst still allowing their adsorption to reactive surfaces, and a separate model analysis was thus performed for each element. By considering the total concentration of the elements one by one, the modelled speciation of the targeted element was less sensitive to the uncertainty resulting from inadequate prediction of the solution concentrations of the other elements (Section S5).

The amount of clay was fixed at 20% based on a previous study on material with the same origin (Gebert and Groengroeft, 2019), with illite being the predominant clay mineral in Elbe sediment (Schulz-Zunkel and Krueger, 2009). Non-specific adsorption to clay was described by a Donnan model similar to Weng et al. (2001) with a charge density of 0.25 eq/kg and an assumed Donnan volume of 0.1 l/kg derived from the properties of illite (McBride, 1994). The acid-base extracted amounts of HA and FA were taken as the total amount of reactive OM in the solid phase. For each pH value, the solution concentrations of HA and FA were subtracted from the total to determine the solid phase amounts of HA and FA after equilibration with the solution. The binding of metal(loid)s to solid and dissolved HA and FA was modelled using the NICA-Donnan model described by Kinniburgh et al. (1996). The generic parameters of Milne et al. (2003) were used for all cations, except for the adsorption parameters of Hiemstra and Van Riemsdijk (2006) for Fe to FA and Xiong et al. (2013) for Pb to both HA and FA. It was assumed that the OM consisted of 50% elemental C.

The concentrations of oxalic acid extracted Fe and Al were combined as a proxy for the total amount of metal (hydr)oxides ($Fe_{AO} + Al_{AO}$). The pH-dependent dissolved amounts of Fe and Al were subtracted from Fe_{AO} and Al_{AO} respectively, to obtain the actual amount of solid (hydr) oxides at each pH. After subtraction, a conversion to total oxide mass was made by assuming 0.68 g Fe/g and 0.35 g Al/g in the (hydr)oxides (Mendez et al., 2020). For the (hydr)oxides, a SSA was calculated as the probe-ion method RSA divided by the mass of converted $Fe_{AO} + Al_{AO}$. This SSA was then attributed to the solid amount of metal (hydr)oxides at each pH, thus describing the pH-dependent total reactive surface area of metal (hydr)oxides in the equilibrated system. Adsorption to the metal (hydr)oxides was modelled using the GTLM submodel for hydrous ferric oxide (Dzombak and Morel, 1990) and the CD-MUSIC submodel for Fh (Hiemstra & Van Riemsdijk, 1996, 2009). For GTLM, parameters for the binding of oxyanions and cations of Dzombak and Morel (1990) were used, with the exception of the binding parameters for MoO_4^- of Gustafsson (2003) and for Pb of Dijkstra et al. (2004). The parameters of Appelo et al. (2002) for Fe^{2+} and CO_3^{2-} were also included. For CD-MUSIC, parameters were taken from the compilation in the Visual MINTEQ Version 4.0 database as applied by Gustafsson and Antelo (2022) and Uddh-Söderberg et al. (2024). The resulting modelled solid-solution partitioning and speciation of elements were evaluated for the two model approaches with either GTLM or CD-MUSIC as the submodel for binding to metal (hydr)oxides. Sensitivities of the model outcomes for specific assumptions are presented in Section S5 and S6, where more details for the individual models are given.

3. Results and discussion

3.1. General properties of the stockpiled sediment

The general properties of the dredged sediment (Table 1) and element concentrations in the 0.43 M HNO_3 (‘reactive’) and 1 mM $CaCl_2$ (‘available’) extracts (Tables S2–S4) were similar between the selected stockpiles. Hence, the (t_0) composition was studied in more detail for a single mixed sample. The C:N ratio was about 10:1 and C comprised 40% of the weight lost by ignition. The IC content converted to $CaCO_3$ suggests the sediment consisted of about 9% carbonates by weight. A substantial amount of reactive S (i.e., 0.43 M HNO_3 extractable) was found (1.4 ± 0.2 g/kg standard deviation) in the stockpiles, likely the remnants of sulphide species oxidised to sulphate during the METHA treatment and stockpiling. The available 1 mM $CaCl_2$ concentration of S was 1.3 (±0.1 g/kg), representing nearly all of the S extracted by 0.43 M HNO_3. The reactive amount of Ca (43 ± 2.7 g/kg or 1.1 mol/kg) is nearly equivalent to the IC concentration (0.9 mol/kg) and therefore mostly originates from calcium carbonate, while sea salt is a likely source of Na (217 ± 21 mg/kg).

3.2. Reactive surfaces quantification and characterisation

The total ‘reactive’ amount of OC assessed by acid-base extraction was 3 g/kg meaning that only 9% of the total OC was extractable (Table 1). The residual OC is generally referred to as humin and is considered less reactive both with regard to mineralisation and metal binding (Hayes and Swift, 2020). A similarly low amount of reactive OC was found in Elbe river sediment by Zander et al. (2023). In contrast, the amount of reactive OM in a broad range of terrestrial soils studied by Dijkstra et al. (2004) varied between 25% and 67%. The short time since aerobic mineralisation of the organic material may explain the relatively low maturation state and development of reactive functional groups of the OM. HA makes up almost half of the acid-base extracted OC, whereas Hy and FA contribute only little to the total OC (Fig. 2). This distribution of the humic fractions in the total sample is very different for soluble OC at low to neutral pH in the pH-stat experiment (Section 3.3), while the distribution and amounts at pH 12 are very similar to the acid-base extraction of the total sample.

Table 2 presents the concentration of Al, Fe, Mn, and P in three extractions targeting different levels of metal (hydr)oxide crystallinity. Al and Fe were higher or equal in oxalic acid compared to dithionite, whereas all three metal concentrations were lower in the ascorbic acid extract. Oxalic acid has often been used to target Al- and Fe oxides with a lower crystallinity than those also extracted with dithionite (e.g., Weng et al., 2001). This difference is not found here, similar to Kostka and Luther (1994) who studied Fe-(hydr)oxides in marsh sediments. The concentrations of metals extracted with ascorbic acid suggests that more than half of the Fe (hydr)oxides were present as nano-crystalline metal (hydr)oxides such as Fh. No substantial difference is found between the concentrations of P in the three extractions, which suggests that almost all PO_4 is adsorbed to the nano-crystalline fraction of the metal (hydr) oxides.

The fitted effective RSA derived with the probe-ion method for the sample is 28 m^2/g (R^2 0.997, 95% confidence interval ± 2.4 m^2/g). This RSA is high compared to a range of agricultural top-soils studied by Mendez et al. (2020), where the RSA varied between 2 and 20 m^2/g. For the (hydr)oxides in the sediment, a combined SSA of 1509 m^2/g is calculated when the RSA is divided by Fe- and Al oxides extracted by oxalic acid (assuming a molar weight of 81.65 g/mol and 78 g/mol respectively). This high SSA suggests a small particle diameter of 1.4 nm for the Fh (Mendez et al., 2020), which may be the result of the short period of formation since the development of oxic conditions in the stockpiled sediment (Hiemstra et al., 2019; Sassi et al., 2024). In line with these findings, the adsorptive properties of the samples were further described by Fh as a proxy for the metal (hydr)oxide fraction. The low reactivity of OM and the high RSA of the metal (hydr)oxides, compared to a range of terrestrial soils (Dijkstra et al., 2004; Mendez

Table 2
Extracted Al-, Fe-, and Mn-(hydr)oxides and co-extracted P from the mixed t_0 sample and the reactive surface area (RSA) for the total sample and specific surface area (SSA) for the oxides.

	Al	Fe	Mn	P	RSA	SSA
	g/kg	g/kg	g/kg	g/kg	m^2/g	m^2/g
Ascorbic acid	0.11	6.44	0.64	1.15	-	-
Oxalic acid	1.03	10.9	0.76	1.19	-	-
Dithionite	0.56	10.6	1.08	1.08	-	-
Probe-Ion	-	-	-	-	28	1509

Table 1
General properties of the six selected stockpiles, ± indicates the standard deviation between the stockpiles. Extended data are provided in Table S1.

pH[a]	EC[b]	θ[c]	LOI[c]	TIC[d]	TOC[d]	OC_{AB}[e]	HA[e]	FA[e]	HY[e]	HON[e]
	µS/cm	%	%	g/kg	g/kg	g/kg	g/kg	g/kg	g/kg	g/kg
7.6	886	69	8.0	11	33	3.0	1.4	0.3	0.2	1.1
(±0.1)	(±66)	(±2.2)	(±0.2)	(±0.8)	(±0.7)					

[a] pH determined in UPW (L/S 10).
[b] EC determined in UPW (L/S 5).
[c] Water content and loss on ignition based on dry weight.
[d] LECO determined total C content.
[e] Acid base extracted OC and humic fractions.

et al., 2020), distinguishes the freshly dredged sediment from previously studied materials and emphasises the relevance of metal (hydr)oxides for contaminant availability in this material.

3.3. pH-dependent solubility of contaminants and surfaces

Fig. 1 shows the pH-stat concentrations for selected metals, concentrations of all analysed elements can be found in Fig. S2. The solution concentrations of most elements vary by several orders of magnitude across the pH-range, typically showing the higher concentrations at both the lower and upper pH and the lowest around neutral pH. This characteristic pH-dependent 'V'- or 'U'-shaped solubility pattern is controlled by pH-dependent adsorption and desorption and by the formation or dissolution of mineral precipitates, as explained further below (Dijkstra et al., 2009; Van Raffe et al., 2025). The modelled solubility and speciation of the elements is consistent with these observations, showing a similarly strong pH-dependence (Fig. 1, Fig. S2). The (oxy) anions (As, Mo, P, and Sb) have a solubility minimum at a lower pH than the cations. The increase of Al and Fe in solution towards both high and low pH is consistent with the dissolution of their metal (hydr)oxides. Not all measured elements have a V- or U-shaped solubility; the solubility of Ba, but especially that of Ca, Sr, and Mg is lowest at the highest pH, Sb has its solubility minimum at pH 2, and the solubility of K and SO_4 show nearly no effect of pH. NH_4^+ exhibits a substantial pH-dependent effect, following a typical V-shape as observed for other elements, despite NH_4^+ being considered to have minimal adsorption to reactive surfaces with a pH-dependent charge such as OM and metal (hydr)oxides (Van Raffe et al., 2025). The solubility of all elements is very similar between the extractions with $CaCl_2$ and UPW. $CaCl_2$ is considered as a more representative solution for soil pore water than UPW (Houba et al., 1990). However, concentrations above 10 mM $CaCl_2$ can cause coagulation of dissolved OM (Weng et al., 2002; Klinkert and Comans, 2020), such effects were virtually absent at 1 mM $CaCl_2$ as was used here.

The dissolved organic carbon (DOC) concentrations show a strong effect of pH (Fig. 2). The dissolution of OM and a marked increase of HA at high pH result from the higher solubility of OM in alkaline solution (Stevenson, 1994). Yet, it should be noted that part of OM may have been coprecipitated with carbonates resulting from the dissolution of atmospheric CO_2 at high pH (Sindelar et al., 2015). Nonetheless, the effect of coprecipitation with carbonates is likely small, because the DOC concentration in the pH-stat extraction at pH 12 is similar to the acid- and base-extracted amount equilibrated without free interaction with the atmosphere (Van Zomeren and Comans, 2007). At a low pH the dissolution of metal (hydr)oxides likely results in the release of mineral-associated OM. This release of mineral-associated OM is largely characterised by an increase in more hydrophilic DOC, particularly FA and Hy (Fig. 2 right panel). This observation might be explained by OM with a relatively high abundance of reactive groups to be preferentially associated with oxides (Kögel-Knabner et al., 2008). The DOC concentrations appear to be higher in the 1 mM $CaCl_2$ solutions compared to UPW, especially at low DOC concentrations around neutral pH. This apparent difference may be caused by differences in storage time (Section 2.4), rather than by Ca-induced effects as observed by Weng et al. (2002) at higher Ca concentrations. Minor degradation of OM may have occurred during this time, potentially leading to slightly higher DOC-concentrations.

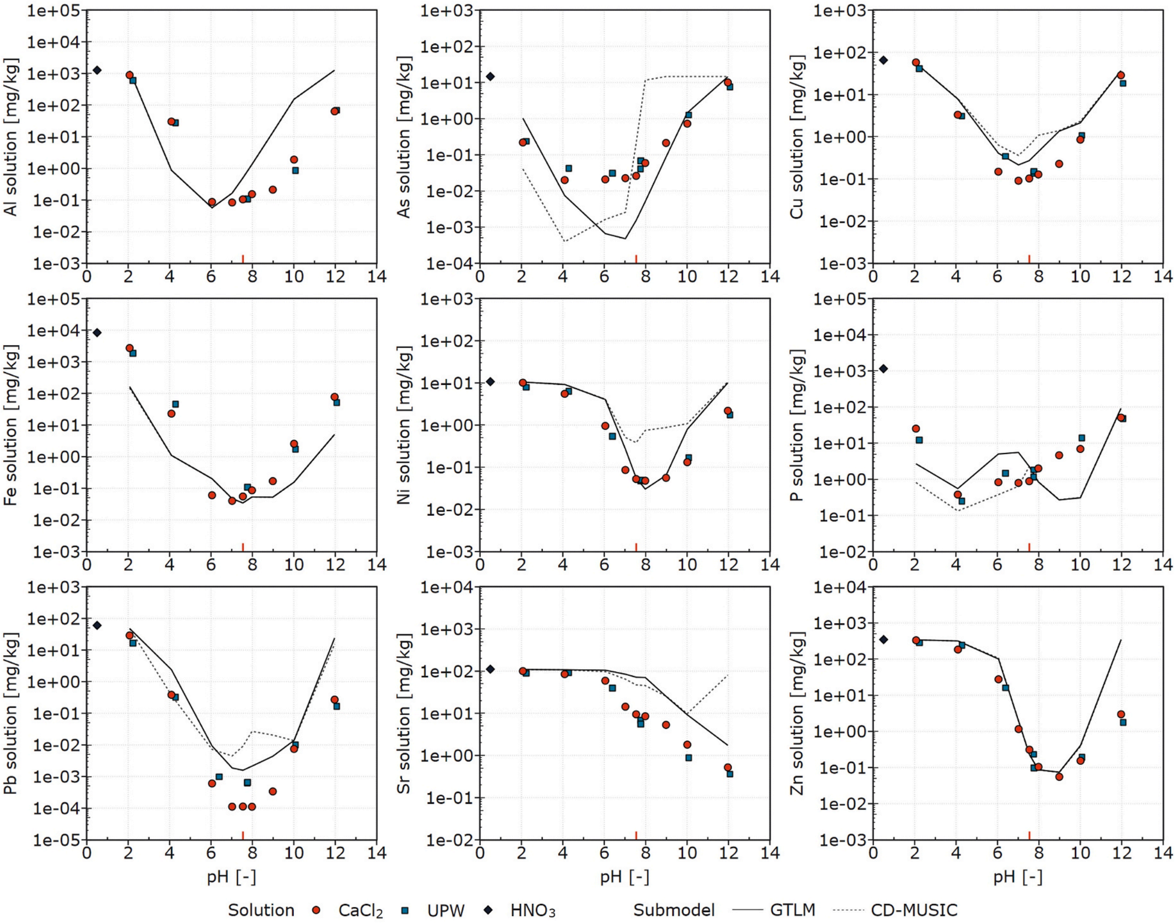

Fig. 1. The measured (points) and modelled (lines) solution amount of selected elements across the pH-range. The 'total reactive amount' extracted with 0.43 M HNO_3 is given at pH 0.5. The red tick mark indicates the sample's natural pH. Other elements are presented in Fig. S2. (For interpretation of the references to color in this figure legend, the reader is referred to the Web version of this article.)

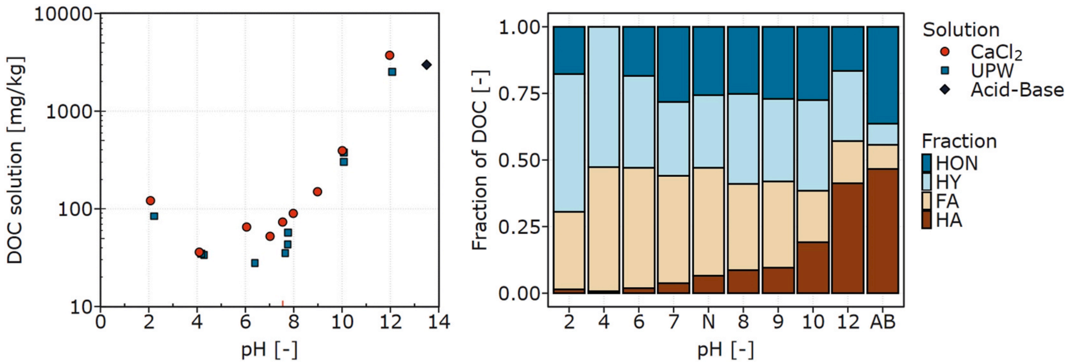

Fig. 2. Left: the pH-dependent amount of dissolved organic carbon (DOC) extracted in ultrapure water (UPW) and 1 mM $CaCl_2$. The acid-base extracted (total reactive) amount of OC is given at pH 13.5. The red tick mark indicates the sample's natural pH. Right: the relative distribution of the operationally defined humic fractions: humic acids (HA), fulvic acids (FA), hydrophilic acids (Hy), and hydrophobic neutrals (HON). (For interpretation of the references to color in this figure legend, the reader is referred to the Web version of this article.)

Noteworthy is the similarity between the solubility at the lowest and highest pH of several metals and that of Fe, Al, and DOC, which suggests that Fe- and Al-(hydr)oxides and OM strongly determine the solid-solution partitioning of metal contaminants in the freshly dredged sediments. This simultaneous release may result either from the dissolution of individual reactive surfaces and associated contaminants and/or from the partial dissociation of organo-mineral complexes, where contaminants bound to the individual surfaces are co-released into the solution. Between pH 6 and 9, Fe, Al, and OM remain mostly in the solid phase and the adsorption of metals to OM and Fe- and Al-(hydr)oxides is controlled by the pH-dependent surface charge and formation of metal hydroxyl species, which result in metal desorption with increasing pH (Van Raffe et al., 2025). In accordance with the observed similarities in solubility, the modelled speciation of many elements is strongly controlled by the pH-dependent adsorption to these reactive surfaces (Fig. 3 and S2). Adsorption to clay was minor for most elements (except Ba, Mg, and Sr) when modelled using a Donnan phase according to the properties of illite (McBride, 1994). It is possible that specific interactions with clays or the presence of other clay minerals, which are not included in this submodel for clay, contributed to the actual solid-solution partitioning of contaminants during the pH-stat extractions.

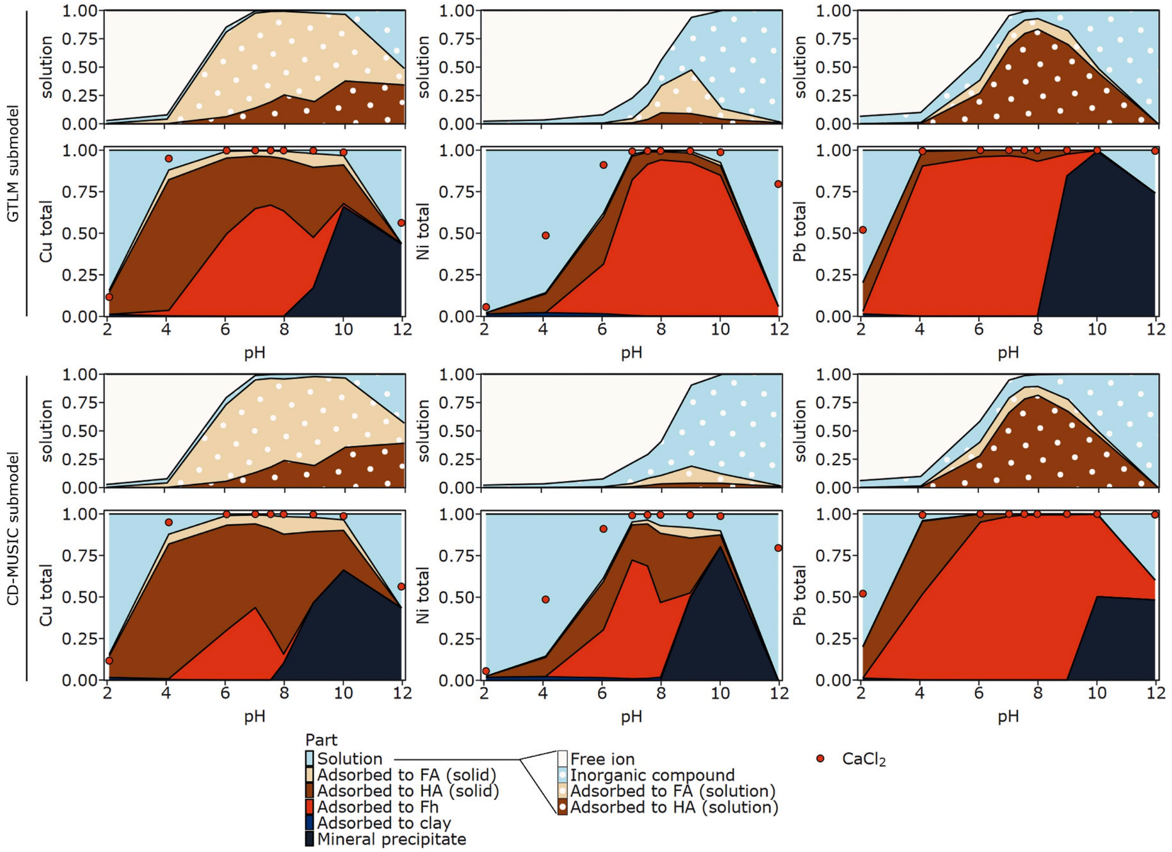

Fig. 3. The modelled solution and total speciation of selected elements across the pH-range. The solution part of the total speciation is specified in the separate solution plots. The solid-solution ratios based on the 1 mM $CaCl_2$ measurements (Fig. 1) are given by the red circles. Top: GTLM as the submodel and bottom: CD-MUSIC as the submodel for the Fe- and Al-(hydr)oxides. Other elements are presented in Fig. S2. (For interpretation of the references to color in this figure legend, the reader is referred to the Web version of this article.)

Fig. 3 and S2 show the modelled speciation distribution based on both the GTLM and CD-MUSIC submodels. At low to intermediate pH a strong association of oxyanions with metal (hydr)oxides is calculated, due to the positive charge of this surface. At higher pH the Fe- and Al-(hydr)oxides become key in the solid-solution partitioning of cations. The solid-solution partitioning of many metals in soils, such as Cu, is often considered to be mostly controlled by OM (Dijkstra et al., 2004; Bonten et al., 2008). However, especially at circumneutral pH, in our dredged sediment a substantial amount of most adsorbed metals is associated with (hydr)oxides as modelled with both GTLM and CD-MUSIC. Still, at pH below 6 and above 9 some cations (i.e., Ba, Cd, Cu, and Sr) are predicted to be strongly controlled by the solid-solution partitioning of OM. Furthermore, at high pH, precipitation of minerals is predicted for several cations (i.e., Ca, Co, Cu, Mg, Ni, Pb, and Zn). Reasons for the large importance of metal (hydr)oxides for binding metal(loids) are likely the high RSA found for the (hydr)oxides and the low reactivity of the OM (Section 3.2). At neutral pH this importance of metal (hydr)oxides is most pronounced, because at this pH the (hydr) oxide surface is most favourably charged for binding metal cations in relation to OM and the solubility of metal (hydr)oxides is lowest.

3.4. Model performance

Equilibrium modelling with generic adsorption parameters is able to predict the solubility of most metal cations (e.g., Cu, Mg, and Ni) adequately (i.e., within 1 log-unit from the measured values). However, at high pH the solution concentration of some cationic metals is overpredicted (i.e., Cd, Mn, Pb, and Zn). This deviation of the modelled solubility of these metals may result from interactions with metal (hydr) oxides at high pH that are not included in the model, such as adsorption of the first hydrolysed species or surface (co)precipitation (Zhu, 2002). Occlusion of cations within the remaining metal (hydr)oxide matrix is unlikely to have affected the measured solution concentrations due to the nano-crystalline nature of the metal (hydr)oxides and their small particle size (Section 3.2). For Al the dissolved concentration is underpredicted at pH 4 and overpredicted at high pH. Gibbsite was used as the mineral for Al in the models, however, the solubility of Al may have been controlled by (secondary) less crystalline Al-(hydr)oxides or multicomponent Al–Fe-(hydr)oxides (Dijkstra et al., 2006; Adams et al., 2021). Supplementary modelling showed that including a solid-solution of Al and Fe was able to improve the model prediction for Al at high pH (Section S6). Using both submodels for adsorption to metal (hydr)oxides, the solution concentrations of As, Mo, and Sb are underpredicted at low to neutral pH. Strong competition of OM for binding to metal (hydr) oxides is expected for (oxy)anions, especially at low pH (Hiemstra et al., 2013;J. Li et al., 2022; Huang et al., 2025). The adsorption of anions at low pH may thus be overestimated in the model, because competition with OM is not accounted for. Moreover, 0.43 M HNO_3 may be unable to fully extract the reactive amount of anions which strongly bind to non-solubilised (hydr)oxides, such as As and Mo (Groenenberg et al., 2017).

It is important to note that the model is based on equilibrium, whereas freshly dredged sediments in the field are subject to long-term oxidative transformation (Vermeulen et al., 2003). Therefore, the quantified and characterised reactive surfaces in this sediment represent the sediment at this ripening stage. Nonetheless, minor changes may have occurred during the 48 h pH-stat extractions due to the meta-stabile nature of the freshly dredged sediment (Dijkstra et al., 2006; Cappuyns et al., 2004). These changes may have included the transformation of the reactive surfaces or partial oxidation of sulphides, which may have affected the solution concentration of metal(loid)s. The model results should therefore be interpreted as a pseudo-equilibrium, providing insight into the processes governing the solid-solution partitioning of the metal(loid)s at a specific ripening stage.

The root of the mean squared error RMSE between the measured and modelled log-concentration of elements in solution is given in Fig. 4. Especially the solid-solution partitioning of the cations Al, Ba, Co, Cr, and Pb appears difficult to predict, indicated by a RMSE of more than one log unit. Of these elements, the RMSE in the natural pH-range (between pH 4 and 9) is higher than the average over the entire pH-range for Co, Cr, and Pb. The modelled speciation of these elements shows near complete adsorption in the solid phase around neutral pH (Fig. S2). However, as the difference between the reactive amount and the solution concentrations span several orders of magnitude, the dissolved concentration in the natural pH-range is not predicted with high accuracy on the log-scale. In addition to this, the generic binding parameters for Cr to OM were estimated without actual adsorption data and are therefore inherently uncertain (Milne et al., 2003; Van Raffe et al., 2025).

The RMSE with the GTLM and CD-MUSIC submodels are similar for most of the elements studied, except for As, Cd, Co, Ni, Pb, Sb, and Sr where the RMSE with CD-MUSIC was higher. The differences for As and Sb are difficult to assess due to the missing competition with OM (see also Section S6). A lower adsorption to Fh is predicted with the CD-MUSIC submodel for Cd, Co, Ni, Pb, and Sr, which results in an overestimation of the amount in solution. This difference between the submodels is most pronounced around neutral pH for Ni and Pb, whereas it is found at a wider pH-range for Cd, Co, and Sr. Sensitivity analysis of the solid-solution partitioning of Cd, Cu, and Zn in soils previously showed little influence of the model binding parameters for metal (hydr)oxides compared to those for OM (Wiersma et al., 2025). However, due to the higher contribution of the metal (hydr)oxides to the adsorption of several elements in our dredged sediment (see also Section S6), such a sensitivity for model parameters and submodels may be more pronounced here. Additional model calculations indicate that the higher accuracy (i.e., lower RMSE-LOG) with the GTLM than CD-MUSIC submodel for some elements (Fig. 4) is unlikely to result from the assumed surface composition of Fh in either model (see Section S6).

For the other elements the multisurface models with either the GTLM or CD-MUSIC submodels predict a more comparable solid-solution

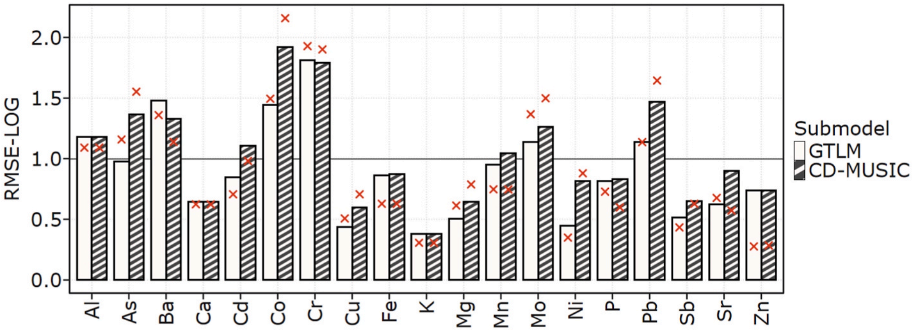

Fig. 4. Root mean square error (RMSE) for the difference between the modelled and measured log amount of each element in solution. The values for the pH-range 2-12 (bars) and pH-range 4-9 (X) are given.

partitioning, especially for Cu, P, Zn, and elements with no or low adsorption to Fh. However, differences in the adsorption to specifically Fh persist for several elements. A lower predicted adsorption with the CD-MUSIC submodel for Fh is partially compensated for and thus masked by a higher adsorption to OM or clay and the formation of precipitates for elements such as Ba, Mg, and Mn (Fig. S2). In addition to this, the dissolution of DOC plays a major part in the solid-solution partitioning of cations as also clearly reflected by the modelled solution speciation. Thus, the predicted solid-solution partitioning is insensitive to the level of mechanistic detail in the submodel for adsorption to metal (hydr)oxides when it is embedded in a multisurface model. This lack of sensitivity makes solid-solution partitioning alone an unsuitable evaluator of submodel performance for this sediment (Oreskes et al., 1994; Kirk Nordstrom, 2012). Additional criteria, such as the free ion concentration (Weng et al., 2001; Koopmans and Groenenberg, 2011) or spectroscopic data (Sjöstedt et al., 2022) have previously been used to constrain a multisurface model. Independent observations of the adsorption specifically to metal (hydr)oxides may enable a direct evaluation which is more sensitive to the selection of the submodel for Fh. In a way, the probe-ion determination of the RSA combined with the CD-MUSIC model, as used here, already serves as an example of modelling a surface specific adsorption phenomenon constrained by independently determined surface properties (Mendez et al., 2020).

CD-MUSIC includes multiple site-specific exchange reactions constrained by the structural composition of the (hydr)oxide surface, thus taking a more physically representative approach to surface complexation than GTLM, which was deliberately developed as "the simplest model that can account qualitatively and quantitatively for all model-constraining experimental data" (Dzombak and Morel, 1990). Moreover, the spatial charge distribution (CD) of surface complexes is considered, rather than simplified to point charges on a single plane as in GTLM (Hiemstra and Van Riemsdijk, 1996; Koopal et al., 2020). The more mechanistic CD-MUSIC model has been shown to explain adsorption of inorganic ions well in controlled systems (e.g., Gustafsson, 2003; Hiemstra et al., 2013; Van Eynde et al., 2022). Due to its fundamental nature, CD-MUSIC has allowed other authors to interpret surface interaction with more complex (natural and synthesised) molecules leading to knowledge development of adsorption phenomena (Z. Li et al., 2022; Xu et al., 2022; Geysels et al., 2025). However, for those elements where differences in the modelled solid-solution partitioning are found for the sediment studied here, the multisurface model with GTLM predicts the solid-solution partitioning of metal(loid)s slightly better (Fig. 4). This difference in performance with the CD-MUSIC submodel may result from a lack of a comprehensive and internally consistent parameter set for a wide range of elements as studied here, such as that for GTLM by Dzombak and Morel (1990) or NICA-Donnan by Milne et al. (2003). Furthermore, the benefit of a more mechanistic model depends increasingly on a precise and complete description of the system. Because such a description is much more challenging in a natural heterogeneous matrix than in a synthetic system, the benefits of more mechanistic modelling are perhaps not fully captured by the modelled solid-solution partitioning alone.

When only aiming to predict the solid-solution partitioning of contaminants, the added value of surface characterisation and mechanistic modelling is thus not apparent. As another example, empirical partition functions have been shown to predict this partitioning well in an environmentally relevant pH-range (Groenenberg et al., 2012). However, purely empirical relationships are inherently constricted by the range of data on which they are based and provide little mechanistic insight. On the contrary, a mechanistic multisurface model as used here is based on more universally applicable assumptions about contaminant speciation and can therefore provide meaningful predictions across a range of conditions while relying on generic and independent parameterisation. Moreover, a mechanistic model represents its underlying conceptual framework, thereby contributing to a comprehensive understanding of the considered processes (Kirk Nordstrom, 2012). From this perspective, the CD-MUSIC model is a better representation of our current understanding about adsorption to metal (hydr)oxides, which is especially relevant in this and other sediments with a dominant role of metal (hydr)oxides dynamics in ion adsorption (Kostka and Luther, 1994). Unfortunately, much of the focus in model assessment is on minimising the quantitative error in prediction, leaving the underlying conceptual framework overlooked (Bredehoeft, 2005). While a sophisticated model such as CD-MUSIC may not yield more accurate numeric predictions, its limitations in performance can more directly reveal processes that are not yet fully understood. Nevertheless, mechanistic modelling of metal(loid) contaminant behaviour makes findings broadly applicable without a loss of predictive quality and therefore has potential for application in environmental risk assessment (e.g. Dijkstra et al., 2018). We therefore expect that the potential release of contaminants during sediment ripening, in which oxide surface are anticipated to play a major role, can be effectively evaluated using a mechanistic modelling approach as applied in this study.

4. Conclusion

The detailed characterisation of reactive mineral and organic surfaces in a freshly dredged sediment showed a high RSA for the metal (hydr)oxides and a low OM reactivity, in comparison to terrestrial soils. The extracted amount of metal(loid)s over a wide pH-range gives valuable input to assess the relevant mechanisms responsible for the availability of contaminants in the sediment. The solubility of most metal contaminants showed a strong pH-effect, with the highest concentrations in solution at the lowest and highest applied pH values. Multisurface geochemical modelling confirmed the relatively high contribution of the metal (hydr)oxides to the adsorption of metal(loid) contaminants. This finding highlights the importance of actual determination of the sediment's metal (hydr)oxide SSA, rather than using an assumed value, for predicting the speciation of these contaminants in this matrix. Comparison of the multisurface model with either the GTLM or CD-MUSIC submodel for ion binding to metal (hydr)oxides showed that, despite its more mechanistic approach, the CD-MUSIC submodel was not found to predict this solid-solution partitioning more accurately than the simplified GTLM model. Nonetheless, the predicted solid-solution partitioning alone may not be a suitable indicator for the benefits of mechanistic models, as this partitioning may be insensitive to the selection of the submodel embedded within the multisurface model. We therefore conclude that the added value of the more detailed mechanistic CD-MUSIC model is in providing a conceptual understanding of relevant processes for contaminant behaviour rather than in more accurate prediction of the solid-solution partitioning.

Overall, we have demonstrated that the detailed characterisation of the properties of the reactive surfaces contributes to more accurate geochemical modelling of the pH-dependent solid-solution partitioning of metal(loid)s compared to commonly used assumptions. Hence, we suggest that temporal changes in contaminant behaviour relevant for the sustainable use of dredged sediments can be more effectively outlined using mechanistic modelling in combination with sample-specific reactive surface characterisation, which will be the subject of a subsequent study.

CRediT authorship contribution statement

Maarten C.J.M. Van Hoef: Conceptualization, Data curation, Formal analysis, Investigation, Methodology, Software, Validation, Visualization, Writing – original draft, Writing – review & editing. **Joris J. Dijkstra:** Conceptualization, Methodology, Supervision, Writing – review & editing. **Rob N.J. Comans:** Conceptualization, Funding acquisition, Project administration, Supervision, Writing – review & editing.

Declaration of competing interest

The authors declare the following financial interests/personal relationships which may be considered as potential competing interests: Maarten van Hoef reports financial support was provided by Dutch Research Council. If there are other authors, they declare that they have no known competing financial interests or personal relationships that could have appeared to influence the work reported in this paper.

Acknowledgement

This publication is part of the project ‘Sediment to Soil’ with file number 18937 of the research programme 2021/TTW/01144385 which is financed by the Dutch Research Council (NWO).

Appendix A. Supplementary data

Supplementary data to this article can be found online at https://doi.org/10.1016/j.apgeochem.2026.106838.

Data availability

Data will be made available on request.

References

Adams, F.T., Machesky, M.L., Kabengi, N., 2021. Surface complexation modeling approach for aluminum-substituted ferrihydrites. ACS Earth Space Chem. 5 (6), 1355–1362. https://doi.org/10.1021/acsearthspacechem.0c00356.

Appelo, C.A.J., Van Der Weiden, M.J.J., Tournassat, C., Charlet, L., 2002. Surface complexation of ferrous iron and carbonate on ferrihydrite and the mobilization of arsenic. Environ. Sci. Technol. 36 (14), 3096–3103. https://doi.org/10.1021/es010130n.

Balkaya, M., 2018. Beneficial use of dredged materials in geotechnical engineering. In: Recycling and Reuse Approaches for Better Sustainability. Springer International Publishing, pp. 21–38. https://doi.org/10.1007/978-3-319-95888-0.

Ball, J.W., Nordstrom, D.K., 2001. User's manual for wateq4f, with revised thermodynamic database and test cases for calculating speciation of major, trace, and redox elements in natural waters. U.S. Geological Survey.

Bastviken, D., Persson, L., Odham, G., Tranvik, L., 2004. Degradation of dissolved organic matter in oxic and anoxic lake water. Limnol. Oceanogr. 49 (1), 109–116. https://doi.org/10.4319/lo.2004.49.1.0109.

Bonten, L.T., Groenenberg, J.E., Weng, L., Van Riemsdijk, W.H., 2008. Use of speciation and complexation models to estimate heavy metal sorption in soils. Geoderma 146 (1–2), 303–310. https://doi.org/10.1016/j.geoderma.2008.06.005.

Bredehoeft, J., 2005. The conceptualization model problem - surprise. Hydrogeol. J. 13 (1), 37–46. https://doi.org/10.1007/s10040-004-0430-5.

Caille, N., Tiffreau, C., Leyval, C., Morel, J.L., 2003. Solubility of metals in an anoxic sediment during prolonged aeration. Sci. Total Environ. 301 (1–3), 239–250. https://doi.org/10.1016/s0048-9697(02)00289-9.

Cappuyns, V., Swennen, R., Devivier, A., 2004. Influence of ripening on pHstat leaching behaviour of heavy metals from dredged sediments. J. Environ. Monit. 6 (9), 774. https://doi.org/10.1039/b406672c.

CEDA, 2019. Sustainable management of the beneficial use of sediments a case-studies review. In: Ceda Information Paper.

Chen, C., Thompson, A., 2017. Ferrous iron oxidation under varying po2 levels: the effect of fe(III)/al(III) oxide minerals and organic matter. Environ. Sci. Technol. 52 (2), 597–606. https://doi.org/10.1021/acs.est.7b05102.

Crocetti, P., González-Camejo, J., Li, K., Foglia, A., Eusebi, A., Fatone, F., 2022. An overview of operations and processes for circular management of dredged sediments. Waste Manag. 146, 20–35. https://doi.org/10.1016/j.wasman.2022.04.040.

Detzner, H.D., Schramm, W., Döring, U., Bode, W., 1998. New technology of mechanical treatment of dredged material from hamburg harbour. Water Sci. Technol. 37 (6–7). https://doi.org/10.1016/s0273-1223(98)00216-9.

Dijkstra, J.J., Meeussen, J.C.L., Comans, R.N.J., 2004. Leaching of heavy metals from contaminated soils: an experimental and modeling Study. Environ. Sci. Technol. 38 (16), 4390–4395. https://doi.org/10.1021/es049885v.

Dijkstra, J.J., Meeussen, J.C.L., Comans, R.N.J., 2009. Evaluation of a generic multisurface sorption model for inorganic soil contaminants. Environ. Sci. Technol. 43 (16), 6196–6201. https://doi.org/10.1021/es900555g.

Dijkstra, J.J., van der Sloot, H.A., Comans, R.N.J., 2006. The leaching of major and trace elements from MSWI bottom ash as a function of pH and time. Appl. Geochem. 21 (2), 335–351. https://doi.org/10.1016/j.apgeochem.2005.11.003.

Dijkstra, J.J., Van Zomeren, A., Brand, E., Comans, R.N., 2018. Site-specific aftercare completion criteria for sustainable landfilling in the Netherlands: geochemical modelling and sensitivity analysis. Waste Manag. 75, 407–414. https://doi.org/10.1016/j.wasman.2018.02.002.

Dzombak, D.A., Morel, F.M.M., 1990. Surface Complexation Modeling: Hydrous Ferric Oxide. John Wiley & Sons.

Frémion, F., Mourier, B., Courtin-Nomade, A., Lenain, J.-F., Annouri, A., Fondanèche, P., et al., 2017. Key parameters influencing metallic element mobility associated with sediments in a daily-managed reservoir. Sci. Total Environ. 605–606, 666–676. https://doi.org/10.1016/j.scitotenv.2017.06.236 (pH-stat, L/S).

Gebert, J., Groengroeft, A., 2019. Long-term hydraulic behaviour and soil ripening processes in a dike constructed from dredged material. J. Soils Sediments 20 (3), 1793–1805. https://doi.org/10.1007/s11368-019-02541-x.

Geysels, B., Hiemstra, T., Groenenberg, J.E., Comans, R.N., 2025. Glyphosate binding and speciation at the water-goethite interface: a surface complexation model consistent with ir spectroscopy and mo/dft. Water Res. 273, 123031. https://doi.org/10.1016/j.watres.2024.123031.

Groenenberg, J.E., Dijkstra, J.J., Bonten, L.T., de Vries, W., Comans, R.N., 2012. Evaluation of the performance and limitations of empirical partition-relations and process based multisurface models to predict trace element solubility in soils. Environ. Pollut. 166, 98–107. https://doi.org/10.1016/j.envpol.2012.03.011.

Groenenberg, J.E., Römkens, P.F.A.M., Van Zomeren, A., Rodrigues, S.M., Comans, R.N., 2017. Evaluation of the single dilute (0.43 M) nitric acid extraction to determine geochemically reactive elements in soil. Environ. Sci. Technol. 51 (4), 2246–2253. https://doi.org/10.1021/acs.est.6b05151.

Groenenberg, J.E., Lofts, S., 2014. The use of assemblage models to describe trace element partitioning, speciation, and fate: a review. Environ. Toxicol. Chem. 33 (10), 2181–2196. https://doi.org/10.1002/etc.2642.

Gustafsson, J.P., 2003. Modelling molybdate and tungstate adsorption to ferrihydrite. Chem. Geol. 200 (1–2), 105–115. https://doi.org/10.1016/s0009-2541(03)00161-x.

Gustafsson, J.P., Antelo, J., 2022. Competitive arsenate and phosphate adsorption on ferrihydrite as described by the cd-music model. ACS Earth Space Chem. 6 (5), 1397–1406. https://doi.org/10.1021/acsearthspacechem.2c00081.

Harmsen, J., 2007. Measuring bioavailability: from a scientific approach to standard methods. J. Environ. Qual. 36 (5), 1420–1428. https://doi.org/10.2134/jeq2006.0492.

Hayes, M.H., Swift, R.S., 2020. Vindication of humic substances as a key component of organic matter in soil and water. In: Advances in Agronomy. Elsevier, pp. 1–37. https://doi.org/10.1016/bs.agron.2020.05.001.

Haynes, R.J., Zhou, Y.-F., 2022. Retention of heavy metals by dredged sediments and their management following land application. In: Advances in Agronomy. Elsevier, pp. 191–254. https://doi.org/10.1016/bs.agron.2021.08.004.

Hiemstra, T., Antelo, J., Rahnemaie, R., Van Riemsdijk, W.H., 2010. Nanoparticles in natural systems I: the effective reactive surface area of the natural oxide fraction in field samples. Geochem. Cosmochim. Acta 74 (1), 41–58. https://doi.org/10.1016/j.gca.2009.10.018.

Hiemstra, T., Mendez, J.C., Li, J., 2019. Evolution of the reactive surface area of ferrihydrite: time, ph, and temperature dependency of growth by ostwald ripening. Environ. Sci. Nano 6 (3), 820–833. https://doi.org/10.1039/c8en01198b.

Hiemstra, T., Mia, S., Duhaut, P.-B., Molleman, B., 2013. Natural and pyrogenic humic acids at goethite and natural oxide surfaces interacting with phosphate. Environ. Sci. Technol. 47 (16), 9182–9189. https://doi.org/10.1021/es400997n.

Hiemstra, T., Van Riemsdijk, W., 1996. A surface structural approach to ion adsorption: the charge distribution (CD) model. J. Colloid Interface Sci. 179 (2), 488–508. https://doi.org/10.1006/jcis.1996.0242.

Hiemstra, T., Van Riemsdijk, W.H., 2006. Biogeochemical speciation of fe in ocean water. Mar. Chem. 102 (3–4), 181–197. https://doi.org/10.1016/j.marchem.2006.03.008.

Hiemstra, T., Van Riemsdijk, W.H., 2009. A surface structural model for ferrihydrite I: sites related to primary charge, molar mass, and mass density. Geochem. Cosmochim. Acta 73 (15), 4423–4436. https://doi.org/10.1016/j.gca.2009.04.032.

Houba, V.J.G., Novozamsky, I., Lexmond, T.M., van der Lee, J.J., 1990. Applicability of 0.01 m cacl2 as a single extraction solution for the assessment of the nutrient status of soils and other diagnostic purposes. Commun. Soil Sci. Plant Anal. 21 (19–20), 2281–2290. https://doi.org/10.1080/00103629009368380.

Huang, Y., Zhao, X., Yang, B., Tang, Y., Zhou, D., Gu, X., 2025. A simple geochemical model for predicting sb(v) partitioning: from iron oxides to complex soil systems. J. Hazard Mater. 496, 139191. https://doi.org/10.1016/j.jhazmat.2025.139191.

ISO 17586, 2016. Soil Quality — Extraction of Trace Elements Using Dilute Nitric Acid.

ISO 12782-1, 2012. Soil quality — parameters for geochemical modelling of leaching and speciation of constituents in soils and materials. Part 1: Extraction of Amorphous Iron Oxides and Hydroxides with Ascorbic Acid.

ISO 12782-2, 2012. Soil Quality — Parameters for Geochemical Modelling of Leaching and Speciation of Constituents in Soils and Materials. *Part 2: Extraction of Crystalline Iron Oxides and Hydroxides with Dithionite*.

ISO 12782-3, 2012. Soil Quality — Parameters for Geochemical Modelling of Leaching and Speciation of Constituents in Soils and Materials. *Part 3: Extraction of Aluminium Oxides and Hydroxides with Ammonium oxalate/oxalic Acid*.

ISO 12782-4, 2012. Soil quality — parameters for geochemical modelling of leaching and speciation of constituents in soils and materials. Part 4: Extraction of Humic Substances from Solid Samples.

ISO 21268-2, 2019. Soil quality — leaching procedures for subsequent chemical and ecotoxicological testing of soil and soil-like materials. Part 2: Batch Test Using a Liquid to Solid Ratio of 10 l/kg Dry Matter.

Jones, A.M., Collins, R.N., Rose, J., Waite, T.D., 2009. The effect of silica and natural organic matter on the fe(ii)-catalysed transformation and reactivity of fe(iii) minerals. Geochem. Cosmochim. Acta 73 (15), 4409–4422. https://doi.org/10.1016/j.gca.2009.04.025.

Kögel-Knabner, I., Guggenberger, G., Kleber, M., Kandeler, E., Kalbitz, K., Scheu, S., et al., 2008. Organo-mineral associations in temperate soils: integrating biology, mineralogy, and organic matter chemistry. J. Plant Nutr. Soil Sci. 171 (1), 61–82. https://doi.org/10.1002/jpln.200700048.

Kim, R.-Y., Yoon, J.-K., Kim, T.-S., Yang, J.E., Owens, G., Kim, K.-R., 2015. Bioavailability of heavy metals in soils: definitions and practical implementation—a critical review. Environ. Geochem. Health 37 (6), 1041–1061. https://doi.org/10.1007/s10653-015-9695-y.

Kinniburgh, D.G., Milne, C.J., Benedetti, M.F., Pinheiro, J.P., Filius, J., Koopal, L.K., Van Riemsdijk, W.H., 1996. Metal ion binding by humic acid: application of the NICA-donnan model. Environ. Sci. Technol. 30 (5), 1687–1698. https://doi.org/10.1021/es950695h.

Kirk Nordstrom, D., 2012. Models, validation, and applied geochemistry: issues in science, communication, and philosophy. Appl. Geochem. 27 (10), 1899–1919. https://doi.org/10.1016/j.apgeochem.2012.07.007.

Klinkert, S., Comans, R.N., 2020. Geochemical multisurface modeling of reactive zinc speciation in compost as influenced by extraction conditions. Environ. Sci. Technol. 54 (4), 2467–2475. https://doi.org/10.1021/acs.est.9b04104.

Koopal, L., Tan, W., Avena, M., 2020. Equilibrium mono- and multicomponent adsorption models: from homogeneous ideal to heterogeneous non-ideal binding. Adv. Colloid Interface Sci. 280, 102138. https://doi.org/10.1016/j.cis.2020.102138.

Koopmans, G.F., Groenenberg, J.E., 2011. Effects of soil oven-drying on concentrations and speciation of trace metals and dissolved organic matter in soil solution extracts of sandy soils. Geoderma 161 (3–4), 147–158. https://doi.org/10.1016/j.geoderma.2010.12.012.

Kostka, J.E., Luther, G.W., 1994. Partitioning and speciation of solid phase iron in saltmarsh sediments. Geochem. Cosmochim. Acta 58 (7), 1701–1710. https://doi.org/10.1016/00167037(94)90531-2.

Li, J., Weng, L., Deng, Y., Ma, J., Chen, Y., Li, Y., 2022. Nom-mineral interaction: significance for speciation of cations and anions. Sci. Total Environ. 820, 153259. https://doi.org/10.1016/j.scitotenv.2022.153259.

Li, Z., Zhao, X., Gu, X., 2022. Thermodynamic and kinetic modeling the interaction of goethite-ligand-metal ternary system. Environ. Pollut. 307, 119462. https://doi.org/10.1016/j.envpol.2022.119462.

Liu, J., Liang, J., Bravo, A.G., Wei, S., Yang, C., Wang, D., Jiang, T., 2021. Anaerobic and aerobic biodegradation of soil-extracted dissolved organic matter from the water-level-fluctuation zone of the three gorges reservoir region, China. Sci. Total Environ. 764, 142857. https://doi.org/10.1016/j.scitotenv.2020.142857.

McBride, M.B., 1994. 3 ion exchange. In: McBride, M.B. (Ed.), Environmental Chemistry of Soils. Oxford University Press, pp. 63–120.

Meeussen, J.C.L., 2003. ORCHESTRA: an object-oriented framework for implementing chemical equilibrium models. Environ. Sci. Technol. 37 (6), 1175–1182. https://doi.org/10.1021/es025597s.

Meima, J.A., Comans, R.N., 1999. The leaching of trace elements from municipal solid waste incinerator bottom ash at different stages of weathering. Appl. Geochem. 14 (2), 159–171. https://doi.org/10.1016/s0883-2927(98)00047-x.

Mendez, J.C., Hiemstra, T., Koopmans, G.F., 2020. Assessing the reactive surface area of soils and the association of soil organic carbon with natural oxide nanoparticles using ferrihydrite as proxy. Environ. Sci. Technol. 54 (19), 11990–12000. https://doi.org/10.1021/acs.est.0c02163.

Milne, C.J., Kinniburgh, D.G., Van Riemsdijk, W.H., Tipping, E., 2003. Generic NICA-donnan model parameters for metal-ion binding by humic substances. Environ. Sci. Technol. 37 (5), 958–971. https://doi.org/10.1021/es0258879.

NEN-EN 14997, 2015. Characterization of waste - leaching behaviour test. Influence of Ph on Leaching with Continuous Ph Control.

Oliveira, B.R.F., Smit, M.P.J., van Paassen, L.A., Grotenhuis, T.C., Rijnaarts, H.H.M., 2016. Functional properties of soils formed from biochemical ripening of dredged sediments—subsidence mitigation in delta areas. J. Soils Sediments 17 (1), 286–298. https://doi.org/10.1007/s11368016-1570-7.

Oreskes, N., Shrader-Frechette, K., Belitz, K., 1994. Verification, validation, and confirmation of numerical models in the earth sciences. Science 263 (5147), 641–646. https://doi.org/10.1126/science.263.5147.641.

OSPAR, 2017. Ospar annual report on dumping and placement of wastes or other matter at sea in 2015. In: Environmental Impacts of Human Activities Series.

Ren, Z.-L., Tella, M., Bravin, M.N., Comans, R.N., Dai, J., Garnier, J.-M., et al., 2015. Effect of dissolved organic matter composition on metal speciation in soil solutions. Chem. Geol. 398, 61–69. https://doi.org/10.1016/j.chemgeo.2015.01.020.

Sassi, M., Qafoku, O., Bowden, M.E., Pearce, C.I., Latta, D., Miller, Q.R.S., et al., 2024. Influence of time and ageing conditions on the properties of ferrihydrite. Environ. Sci. Nano 11 (4), 1682–1692. https://doi.org/10.1039/d3en00828b.

Schulz-Zunkel, C., Krueger, F., 2009. Trace metal dynamics in floodplain soils of the river elbe: a review. J. Environ. Qual. 38 (4), 1349–1362. https://doi.org/10.2134/jeq2008.0299.

Sindelar, H.R., Brown, M.T., Boyer, T.H., 2015. Effects of natural organic matter on calcium and phosphorus co-precipitation. Chemosphere 138, 218–224. https://doi.org/10.1016/j.chemosphere.2015.05.008.

Sjöstedt, C., Kristofferson, Å., Gustafsson, J.P., Heldele, A.-S., Kessler, V., Kleja, D.B., 2022. Evidence of the mineral znhaso4·h2o, koritnigite, controlling as(v) and zn(ii) solubility in a multi-contaminated soil. Appl. Geochem. 140, 105301. https://doi.org/10.1016/j.apgeochem.2022.105301.

Stevenson, F.J., 1994. Humus Chemistry, second ed. ed. John Wiley, New York (Includes bibliographical references and index).

Swift, R.S., 1996. Organic matter characterization. In: Methods of Soil Analysis. John Wiley & Sons, Ltd, pp. 1011–1069. https://doi.org/10.2136/sssabookser5.3.c35.

Tipping, E., Rieuwerts, J., Pan, G., Ashmore, M.R., Lofts, S., Hill, M.T.R., et al., 2003. The solid–solution partitioning of heavy metals (Cu, Zn, Cd, Pb) in upland soils of England and Wales. Environ. Pollut. 125 (2), 213–225. https://doi.org/10.1016/S0269-7491(03)00058-7.

Uddh-Söderberg, T., Augustsson, A., Kleja, D.B., Jarsjö, J., Fröberg, M., Åström, M., Gustafsson, J.-P., 2024. Challenges in geochemical modelling of metal(loid) solubility and binding mechanisms along a soil profile at a multi-contaminated site. Appl. Geochem. 170, 106063. https://doi.org/10.1016/j.apgeochem.2024.106063.

US-EPA, 1999. Minteqa2/prodefa2, a geochemical assessment model for environmental systems: user manual supplement for version 4.0. National Exposure Research Laboratory Ecosystems Research Division.

Van Eynde, E., Hiemstra, T., Comans, R.N., 2022. Interaction of zn with ferrihydrite and its cooperative binding in the presence of po4. Geochem. Cosmochim. Acta 320, 223–237. https://doi.org/10.1016/j.gca.2022.01.010.

Van Raffe, F., Dijkstra, J.J., Comans, R.N., 2025. Mechanisms controlling the release of inorganic contaminants, organic matter fractions, and ammonium from solid landfill waste: ph dependent leaching experiments and geochemical modelling. Appl. Geochem. 190, 106503. https://doi.org/10.1016/j.apgeochem.2025.106503.

Van Zomeren, A., Comans, R.N.J., 2007. Measurement of humic and fulvic acid concentrations and dissolution properties by a rapid batch procedure. Environ. Sci. Technol. 41 (19), 6755–6761. https://doi.org/10.1021/es0709223.

Vermeulen, J., Grotenhuis, T., Joziasse, J., Rulkens, W., 2003. Ripening of clayey dredged sediments during temporary upland disposal a bioremediation technique. J. Soils Sediments 3 (1), 49–59. https://doi.org/10.1007/bf02989469.

Vermeulen, J., van Gool, M.P., Dorleijn, A.S., Joziasse, J., Bruning, H., Rulkens, W.H., Grotenhuis, J.T., 2007. Biochemical ripening of dredged sediments. part 1. kinetics of biological organic matter mineralization and chemical sulfur oxidation. Environ. Toxicol. Chem. 26 (12), 2530. https://doi.org/10.1897/06-545.1.

Weng, L., Temminghoff, E.J., Van Riemsdijk, W.H., 2002. Interpretation of humic acid coagulation and soluble soil organic matter using a calculated electrostatic potential. Eur. J. Soil Sci. 53 (4), 575–588. https://doi.org/10.1046/j.1365-2389.2002.00455.x.

Weng, L., Temminghoff, E.J.M., Van Riemsdijk, W.H., 2001. Contribution of individual sorbents to the control of heavy metal activity in sandy soil. Environ. Sci. Technol. 35 (22), 4436–4443. https://doi.org/10.1021/es010085j.

Wiersma, W., Van Eynde, E., Comans, R.N.J., Groenenberg, J.E., 2025. Quantifying the accuracy, uncertainty, and sensitivity of soil geochemical multisurface models. Environ. Sci. Technol. 59 (10), 5172–5181. https://doi.org/10.1021/acs.est.4c04812.

Xiong, J., Koopal, L.K., Tan, W., Fang, L., Wang, M., Zhao, W., et al., 2013. Lead binding to soil fulvic and humic acids: Nica-donnan modeling and xafs spectroscopy. Environ. Sci. Technol. 47 (20), 11634–11642. https://doi.org/10.1021/es402123v.

Xu, Y., Hiemstra, T., Tan, W., Bai, Y., Weng, L., 2022. Key factors in the adsorption of natural organic matter to metal (hydr)oxides: fractionation and conformational change. Chemosphere 308, 136129. https://doi.org/10.1016/j.chemosphere.2022.136129.

Zander, F., Comans, R., Gebert, J., 2023. Linking patterns of physical and chemical organic matter fractions to its lability in sediments of the tidal elbe river. Appl. Geochem. 156, 105760. https://doi.org/10.1016/j.apgeochem.2023.105760.

Zhu, C., 2002. Estimation of surface precipitation constants for sorption of divalent metals onto hydrous ferric oxide and calcite. Chem. Geol. 188 (1–2), 23–32. https://doi.org/10.1016/s00092541(02)00060-8.